

Development of Broadband Cavity Ring-Down Spectroscopy for Biomedical Diagnostics of Liquid Analytes

S.-S. Kiwanuka,[†] T. K. Laurila,^{†,§,||} J. H. Frank,[⊠] A. Esposito,[⊗] K. Blomberg von der Geest,[○] L. Pancheri,[#] D. Stoppa,[#] and C. F. Kaminski^{*,†,‡}

[†]Department of Chemical Engineering and Biotechnology, University of Cambridge, Pembroke Street, Cambridge CB2 3RA, U.K.

[‡]SAOT School of Advanced Optical Technologies, Max Planck Institute for the Science of Light, University of Erlangen-Nuremberg, Guenther-Scharowsky-Strasse 1, D-91058 Erlangen, Germany

[§]Metrology Research Institute, Aalto University, Espoo, Finland

^{||}Centre for Metrology and Accreditation (MIKES), Espoo, Finland

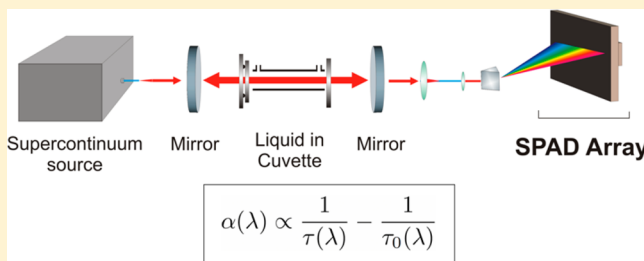
[⊠]Combustion Research Facility, Sandia National Laboratories, Livermore California 94551, United States

[⊗]Medical Research Council Cancer Cell Unit, Hutchison/MRC Research Centre, Cambridge, U.K.

[○]Unit of Measurement Technology, Cemis-Oulu, University of Oulu, Finland

[#]Fondazione Bruno Kessler (FBK), Trento, Italy

ABSTRACT: We present a spectrometer for sensitive absorption measurements in liquids across broad spectral bandwidths. The spectrometer combines the unique spectral properties of incoherent supercontinuum light sources with the advantages of cavity ring-down spectroscopy, which is a self-calibrating technique. A custom-built avalanche photodiode array is used for detection, permitting the simultaneous measurement of ring-down times for up to 64 different spectral components at nanosecond temporal resolution. The minimum detectable absorption coefficient was measured to be $3.2 \times 10^{-6} \text{ cm}^{-1} \text{ Hz}^{-1/2}$ at 527 nm. We show that the spectrometer is capable of recording spectral differences in trace levels of blood before and after hemolysis.



The precise quantification of concentrations of chemical species is key to many applications in science and industry. Single-pass optical absorption spectroscopy provides the simplest method of quantification, but its sensitivity is typically limited to absorbance changes in the 10^{-3} range.¹ The sensitivity can be improved by many orders of magnitude through use of optical cavities to increase the absorption path length permitting the detection of trace species. One popular cavity-enhanced method is cavity ring-down spectroscopy (CRDS), as first demonstrated by O'Keefe & Deacon.² In CRDS, a pulse of light is coupled into a high-finesse two-mirror cavity. The pulse intensity decreases with each round-trip due to sample absorption and mirror losses. The rate of intensity decay of light within the cavity can be measured (yielding the so-called ring-down time), from which the absorber concentration can be quantified. The CRDS technique is sensitive, immune to intensity noise in the excitation source and self-calibrating.

Until recently, CRDS measurements over wide spectral ranges, i.e., measurement of multiple species at once, have been limited because of the requirement to resolve multiple ring-down times in parallel and due to the unavailability of pulsed, broad bandwidth sources with sufficient brightness.³ Sources that have traditionally been used in optical cavity techniques,

such as tunable lasers,⁴ filament lamps,^{5,6} and light emitting diodes (LEDs),^{7,8} suffer from low spectral power density and/or limited spectral bandwidths. However, the recent advent of high brightness optical frequency combs^{9,10} and supercontinuum (SC) sources¹¹ is leading to a paradigm shift in the field.^{12,13}

We have recently shown that broad bandwidth incoherent supercontinua^{14,15} are particularly well suited for many different applications in the CRDS-related technique of broad bandwidth cavity-enhanced absorption spectroscopy (CEAS).¹⁶ Recent demonstrations of broadband SC-CEAS include the monitoring of reactions in liquid solution,¹⁷ analysis of atmospheric species in the gas phase,¹⁸ and the detection of electrogenerated species at interfaces within a thin layer cell.^{19,20} In SC-CEAS, incoherent SC light is coupled into the optical cavity and the requirement for longitudinal mode-matching is relaxed. In contrast to frequency comb techniques,²¹ SC-CEAS is therefore simpler to set up and more robust, while featuring comparable

Received: April 27, 2012

Accepted: June 1, 2012

Published: June 1, 2012

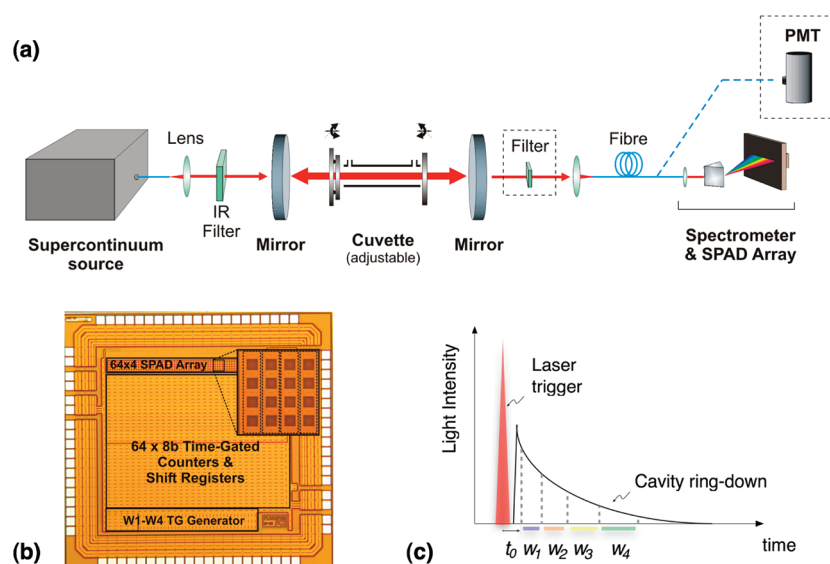


Figure 1. (a) Experimental BB-CRDS setup for the study of liquid analytes. A commercial pulsed supercontinuum radiation source produces broadband light which is coupled into the optical cavity formed by a pair of plano-concave mirrors. The optical cavity is used to pass light multiple times through the liquid sample contained in the 5.4 cm long intracavity cuvette (2.7 mL volume). Transmitted light is dispersed through a spectrometer onto the time-gated SPAD array detector. A PMT arm was used to compare results with a narrowband single-channel CRDS measurement for a filtered portion of the output. (b) Micrograph of the SPAD array chip. Each of the 64 spectral elements can be time gated in rapid succession (gates w_1 to w_4) and consists of four light sensitive SPADs which are read out in parallel. (c) The signal ring-down time is determined from integrated signals during gates w_1 to w_4 .

detection sensitivities, crucial advantages to establish the technique for applications in the field.

The disadvantage of broadband CEAS is the need for a separate calibration measurement, as the mirror reflectivity must be accurately determined at each individual wavelength position.²² CRDS does not suffer this disadvantage, and successful implementations of CRDS with broadband light sources have been reported. Ball et al.²³ and Scherer et al.²⁴ have used a clocked charge coupled device (CCD) to capture spectral information and ring-down times in parallel. Thorpe et al. locked the modes of an optical frequency comb to the eigenmodes of an optical cavity and used a scanning mirror streak camera for detection.²¹ Both of these technologies are suited for trace level measurements in the gas phase, where use of high finesse cavities results in long ring-down times (on the microsecond time scale), but they are too slow for applications in the liquid phase,¹⁷ where ring-down times may be as short as a few nanoseconds. Therefore, the simultaneous resolution of multiple ring-down times, particularly in liquids, remains a challenge.

In this work, we overcome these problems and report on the implementation of broadband CRDS (BB-CRDS) with a pulsed incoherent supercontinuum as a broadband excitation source and a novel CMOS-based single photon avalanche photodiode (SPAD) array²⁵ for the simultaneous detection of ring-down times in 64 separate spectral channels. The use of CMOS technology enables on-chip processing, e.g., time-gating, which is a major advantage. The sensitivity and temporal resolution of the developed technique permit novel quantitative assays to be developed for liquid samples, combining sensitivities approaching those of fluorescence techniques, with the ease of quantification offered by direct absorption measurements. We develop the technique into a sensitive spectrometer capable of detecting spectral differences between whole and lysed blood present in solution at trace concentrations.

EXPERIMENTAL SECTION

The setup of the broadband CRD spectrometer is shown in Figure 1a. We used a commercial supercontinuum source (Fianium SC-390) operated at a 1 MHz pulse repetition rate and 3 W average power in the wavelength range from 390 to 2400 nm. A hot mirror (Comar 716 GK 25) was used to limit the output to visible wavelengths. The light was coupled into a 42 cm optical cavity formed by a pair of plano-concave mirrors (Layertec, 0.5 m radius of curvature, 99.0% nominal reflectivity between 400 and 680 nm). The liquid analyte was contained in a custom-designed 5.4 cm cuvette placed inside the optical cavity as described previously.¹⁷ The use of higher reflectivity mirrors would not yield greater sensitivity as the absorption length in liquid samples is limited by intracavity losses due to solvent extinction²⁶ and the presence of cuvette windows.¹⁷ Light transmitted through the cavity was coupled into a multimode fiber (Thorlabs GIF 625) and dispersed and focused onto the SPAD array to record individual cavity ring-down signals in 64 spectral channels. The custom-built spectrometer comprised of a lens ($f = 6$ mm), dispersion prism (Edmund Optics SF11, MgF₂ 25 mm glass), and a focusing lens (achromatic doublet, $f = 20$ mm). A photomultiplier tube (PMT, Hamamatsu R636-10) was used to record narrowband single-channel CRDS measurements for comparison and validation of the technique. In this case, a spectral filter was used to select the desired region of interest.

The SPAD array is implemented in CMOS technology. The four SPADs in each of the 64-spectral elements operate in parallel, working as a single vertical spectral pixel (see Figure 1b). Signals from all four SPADs are binned and then processed by 8-bit time-gated counters featured on the chip, performing the photon counting along four consecutive time windows. The individual widths of the time gates w_1 – w_4 are adjustable between 0.7 and 10 ns (see Figure 1c). The SPAD array received trigger signals from a pulse generator (Agilent

33521A) to set an initial time delay, t_0 , with respect to the pump laser pulse. Adjustment of t_0 permits different sections along the exponential ring-down decay to be sampled. The signal from each time-gate was averaged for 0.1 s ($\sim 100\,000$ shots) before the SPAD array was read out. Further technical details on the SPAD array electronics, specifications, and operation can be found in a previous publication by Pancheri and Stoppa.²⁵ The width w_n and time point t_n of the four time gates were measured from the detector response to a short input laser pulse (<200 ps) at different time delays t_0 .

The ring-down times, τ , were determined at each of the 64 spectral channels in the presence (τ) and absence (τ_0) of the absorbing sample. The absorbance, A , was then calculated according to¹

$$A(\lambda) = \frac{\alpha(\lambda)d}{2.303} = \frac{L}{2.303c} \left[\frac{1}{\tau(\lambda)} - \frac{1}{\tau_0(\lambda)} \right] \quad (1)$$

where c is the speed of light, L is the optical length of the cavity, α is the sample absorption coefficient, and d the optical length inside the liquid sample. Note $L = L_{\text{air}}n_{\text{air}} + dn_{\text{liquid}}$, where L_{air} is the free-space intracavity length in air and n represents the related refractive indices. Equation 1 is valid for $\alpha \ll 1$.

RESULTS AND DISCUSSION

The ability of the BB-CRDS technique to correctly sample different portions of a ring-down curve was first determined. The decay time, τ , is calculated from $\ln I_n/I_0 = -1/\tau t_n$ for each spectral element or pixel. Figure 2a shows a plot of $\ln(I_n)$ vs

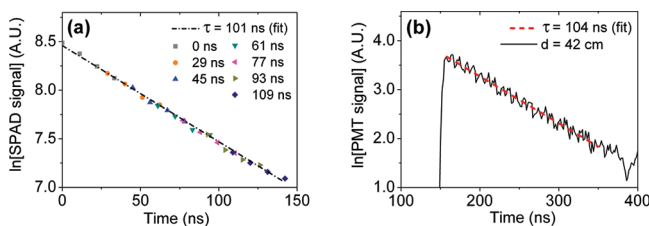


Figure 2. Cavity ring-down measurements of pure water using a 70 nm band-pass filter centered at 500 nm. (a) Composite semilog decay plot of SPAD array data obtained for different laser trigger time delays t_0 . For each t_0 , 4 individual data points are obtained (corresponding to w_1 to w_4). Each data point corresponds to spectral averages across all pixels over 250 shots. (b) Corresponding ring-down trace obtained with a PMT detector.

time obtained by adjusting the initial laser trigger time delay t_0 (see Figure 1c). By linear fitting of the slope, one obtains $\tau = 101 \pm 5$ ns. For validation, the signal decay was also measured with a photomultiplier tube (PMT, Hamamatsu R636-10) and an 8 GHz bandwidth digital oscilloscope (Tektronix TDS6804B). The ring-down time obtained with the PMT was 104 ± 1.8 ns (see Figure 2b), yielding agreement to within 4%. For both SPAD and PMT measurements, parts a and b of Figure 2, respectively, the bandwidth of the transmitted light was filtered to a width of 70 nm centered around 500 nm.

The detection limit was estimated from measurements of various concentrations of Rhodamine 6G (Rh6G, Sigma Aldrich, $\epsilon = 116\,000 \text{ M}^{-1} \text{ cm}^{-1}$ at 529.75 nm) dissolved in ultrapure water ($18 \text{ M}\Omega \text{ cm}^{-1}$, Milli-Q, Millipore). A linear absorption response ($R^2 > 0.99$) was obtained for concentrations between 17.6 and 142.9 nM ($10^{-9} \text{ mol L}^{-1}$). Taking the standard deviation of the baseline noise to be the minimum

detectable absorption coefficient, α_{min} , yields a value of $\alpha_{\text{min}} = 3.2 \times 10^{-6} \text{ cm}^{-1} \text{ Hz}^{-1/2}$ at a spectral resolution of 0.7 nm per pixel.

Using the definition $\text{LOD} = 3 \alpha_{\text{min}}/2.303\epsilon$ as described by Seetohul et al.²⁷ gives a minimum detectable limit of detection, LOD, of 120 pM. These figures are comparable with results achieved using single-wavelength liquid-phase CRDS techniques^{20,28} and also close to what the current authors previously reported using broadband CEAS in liquids.¹⁷ Here we achieve an effective increase in path length of approximately 50 times the cuvette length. Figure 3 shows BB-CRDS spectra of

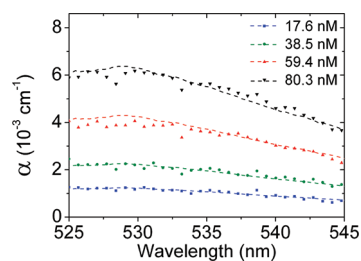


Figure 3. Broadband CRDS spectra of Rhodamine 6G at concentrations ranging from 17.6 to 80.3 nM in $18 \text{ M}\Omega \text{ cm}^{-1}$ ultrapure water. Signal integration times were 100 ms, corresponding to $\sim 100\,000$ individual supercontinuum pulses. Dashed lines represent reference spectra obtained with SC-CEAS.¹⁷

Rhodamine 6G and, for comparison, broadband SC-CEAS measurements, as described in Kiwanuka et al.¹⁷ The general agreement between these independent measurement techniques is very good although some wavelength-dependent systematic differences can be seen, likely resulting from differences in the relative pixel sensitivities and spectral throughput between the two approaches.

The inherently self-calibrating nature and substantial increase in sensitivity over single-pass absorption techniques make BB-CRDS attractive for a number of liquid-phase applications. One such example is the analysis of blood at low concentration. Blood contains many important physiological components, but its spectroscopic properties are dominated by hemoglobin (Hb) and spectra vary according to the oxygenation state of the heme group in Hb.^{29,30} Co-oximetry^{31,32} and photometry^{33,34} are the routine methods for Hb analysis in blood and are popular due to their portability, small sample volume, relatively low cost, and simplicity. However, their limited sensitivity only allows Hb tetramer concentrations of 50–150 g/L to be detected. Furthermore, their application requires hemolysis of blood cells prior to measurement and their spectral resolution is limited. The development of a more sensitive method for quantifying blood concentration with the ability to monitor variations in composition by measuring changes in absorption spectra at trace levels would constitute a significant advance in biomedical diagnostic capabilities.

Figure 4a shows spectra of both whole blood (at 2.7×10^{-2} g/L tetramer concentration, corresponding to 5×10^4 RBC/mL concentration) and lysed blood (at 1.35×10^{-2} g/L tetramer or 1×10^5 RBC/mL concentration) acquired using the BB-CRDS technique. The blood samples were obtained from healthy volunteers by venipuncture into a syringe with heparin after informed, written consent. Whole blood was diluted with 50% RPMI-1640 buffer solution. Hemolysis was achieved osmotically with samples diluted in ultrapure ($18 \text{ M}\Omega \text{ cm}^{-1}$) water from 50% hematocrit. In complex media such as

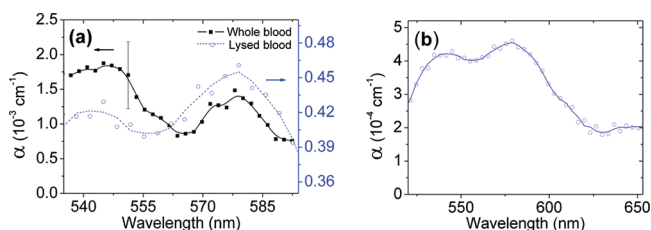


Figure 4. (a) BB-CRDS spectra of whole blood at 5×10^4 RBC/mL concentration and lysed blood at 1×10^5 RBC/mL concentration. Data are an average of 20 spectra acquired at 10 Hz. The error bar included represents the uncertainty (1σ) associated with the linear fit to the four data points of each spectral channel and is representative for all other data points shown. (b) Spectrum of lysed blood at 1×10^5 RBC/mL concentration spanning 130 nm. Data are fitted with a 5-point Savitzky–Golay convolution for visualization (solid and dashed lines). Spectral data were acquired at a resolution of 2 nm per pixel for whole blood and 3.3 nm per pixel for lysed blood.

blood, scattering from suspended particulates can present a problem and filtering to remove large particulate matter prior to conducting an absorption experiment may be beneficial. For the low dilution ratios used in the present experiments, such effects are however negligible as was previously shown in Horecker et al.²⁹ The technique presented here can be used to detect spectral differences in absorption features. Spectra shown in Figure 4 were integrated over 2 s. Detection limits of 1.5×10^4 RBC/mL for whole blood and 5.8×10^4 RBC/mL for lysed blood, respectively, were obtained. Note that even higher sensitivity could be achieved by shifting the excitation wavelength to 415 nm, which lies in the Soret excitation band of hemoglobin and features an approximately 10-fold increase in the absorption cross section. In our present setup this potential improvement could not be realized because of power limitation in the available light source. A spectrum of lower resolution but featuring broader wavelength coverage of 130 nm across the pixel array is also shown (Figure 4b). It corresponds to lysed blood at 1×10^5 RBC/mL concentration and was obtained during 2 s of integration.

CONCLUSIONS

We demonstrate the development of BB-CRDS with incoherent supercontinua for the analysis of liquid analytes at trace concentrations. The method offers good sensitivity with high spectral resolution and is self-referencing, obviating the need for extensive calibration protocols. We anticipate many potential applications ranging from medical diagnostics, ranging from blood-based medical assays to applications in the basic sciences and process industries. We demonstrate these advantages via the sensitive detection of blood as a potential application in medical analysis, e.g., for urinalysis and also in forensic studies. The technique could be developed into a flexible and cost-effective sensor technology due to the scalability of CMOS production techniques. We envisage future enhancements in CMOS-based SPAD detector technology to lead to sensitivity improvements, for example, improved fill factors achieved through microlens arrays and better performance through increases in the number of time-gates and photosensitive pixels.

AUTHOR INFORMATION

Corresponding Author

*E-mail: cfk23@cam.ac.uk. Phone: +44 (0)1223 (3)30133. Fax: +44 (0)1223 334796.

Notes

The authors declare no competing financial interest.

ACKNOWLEDGMENTS

C.F.K. acknowledges funding from EPSRC under Grant EP/H018301/1. A.E. is funded by the EPSRC (Grant EP/F044011). T.K.L. acknowledges the financial support from the Academy of Finland. K.B.v.d.G. and T.K.L. acknowledge financial support from the Finnish Funding Agency for Technology and Innovation. J.H.F. acknowledges support from the U.S. Department of Energy, Office of Basic Energy Sciences, Division of Chemical Sciences, Geosciences, and Biosciences. This research was supported by a Marie Curie European Reintegration Grant within the 7th European Community Framework Programme. We wish to acknowledge Drs. T. Tiffert and V. L. Lew (Department of Physiology, Development and Neuroscience, University of Cambridge) for providing the blood samples and for helpful advice.

REFERENCES

- (1) Lehmann, K. K.; Berden, G.; Engeln, R. In *Cavity Ring-Down Spectroscopy*; John Wiley & Sons, Ltd.: Chichester, U.K., 2010; pp 1–26.
- (2) O’Keefe, A.; Deacon, D. A. G. *Rev. Sci. Instrum.* **1988**, *59*, 2544–2551.
- (3) Ball, S. M.; Jones, R. L. *Chem. Rev.* **2003**, *103*, 5239–5262.
- (4) Hult, J.; Burns, I. S.; Kaminski, C. F. *Appl. Opt.* **2005**, *44*, 3675–3685.
- (5) Fiedler, S. E.; Hese, A.; Ruth, A. A. *Chem. Phys. Lett.* **2003**, *371*, 284–294.
- (6) Hamers, E.; Schram, D.; Engeln, R. *Chem. Phys. Lett.* **2002**, *365*, 237–243.
- (7) Kebabian, P. L.; Herndon, S. C.; Freedman, A. *Anal. Chem.* **2005**, *77*, 724–728.
- (8) Kebabian, P. L.; Robinson, W. A.; Freedman, A. *Rev. Sci. Instrum.* **2007**, *78*, 063102.
- (9) Udem, T.; Holzwarth, R.; Hansch, T. W. *Nature* **2002**, *416*, 233–237.
- (10) Cundiff, S.; Ye, J. *Rev. Mod. Phys.* **2003**, *75*, 325–342.
- (11) Alfano, R. R. *The Supercontinuum Laser Source*, 2nd ed.; Springer-Verlag: New York, 2006.
- (12) Stelmaszczyk, K.; Rohwetter, P.; Fechner, M.; Queifler, M.; Czyzewski, A.; Stacewicz, T.; Wöste, L. *Opt. Express* **2009**, *17*, 3673–3678.
- (13) Stelmaszczyk, K.; Nakaema, W. M.; Hao, Z.-q.; Rohwetter, P.; Wöste, L. *Sensors* **2011**, 11–12.
- (14) Liu, C.; Rees, E. J.; Laurila, T.; Jian, S.; Kaminski, C. F. *Opt. Express* **2010**, *18*, 26113–26122.
- (15) Liu, C.; Rees, E. J.; Laurila, T.; Jian, S.; Kaminski, C. F. *Opt. Express* **2012**, *20*, 6316–6324.
- (16) Kaminski, C. F.; Watt, R. S.; Elder, A. D.; Frank, J. H.; Hult, J. *Appl. Phys. B: Laser Opt.* **2008**, *92*, 367–378.
- (17) Kiwanuka, S.-S.; Laurila, T.; Kaminski, C. F. *Anal. Chem.* **2010**, *82*, 7498–7501.
- (18) Langridge, J. M.; Laurila, T.; Watt, R. S.; Jones, R. L.; Kaminski, C. F.; Hult, J. *Opt. Express* **2008**, *16*, 10178–10188.
- (19) Schnippering, M.; Unwin, P. R.; Hult, J.; Laurila, T.; Kaminski, C. F.; Langridge, J. M.; Jones, R. L.; Mazurenka, M.; Mackenzie, S. R. *Electrochem. Commun.* **2008**, *10*, 1827–1830.
- (20) van der Sneppen, L.; Hancock, G.; Kaminski, C.; Laurila, T.; Mackenzie, S. R.; Neil, S. R. T.; Peverall, R.; Ritchie, G. A. D.; Schnippering, M.; Unwin, P. R. *Analyst* **2010**, *135*, 133–139.

- (21) Thorpe, M. J.; Moll, K. D.; Jones, R. J.; Safdi, B.; Ye, J. *Science* **2006**, *311*, 1595–1599.
- (22) Laurila, T.; Burns, I. S.; Hult, J.; Miller, J. H.; Kaminski, C. F. *Appl. Phys. B: Laser Opt.* **2011**, *102*, 271–278.
- (23) Ball, S. M.; Povey, I. M.; Norton, E. G.; Jones, R. L. *Chem. Phys. Lett.* **2001**, *342*, 113–120.
- (24) Scherer, J. J.; Paul, J. B.; Jiao, H.; O’Keefe, a. *App. Opt.* **2001**, *40*, 6725–6732.
- (25) Pancheri, L.; Stoppa, D. *2009 Proc. ESSCIRC* **2009**, 428–431.
- (26) Pope, R. M.; Fry, E. S. *Appl. Opt.* **1997**, *36*, 8710–8723.
- (27) Seetohul, L. N.; Ali, Z.; Islam, M. *Analyst* **2009**, *134*, 1887–1895.
- (28) Xu, S.; Sha, G.; Xie, J. *Rev. Sci. Instrum.* **2002**, *73*, 255–258.
- (29) Horecker, B. L. *J. Biol. Chem.* **1943**, *1*, 173–183.
- (30) Rother, R. P.; Bell, L.; Hillmen, P.; Gladwin, M. T. *JAMA, J. Am. Med. Assoc.* **2005**, *293*, 1653.
- (31) Vreman, H. J.; Mahoney, J. J.; Van Kessel, a. L.; Stevenson, D. K. *Clin. Chem.* **1988**, *34*, 2562–2566.
- (32) Zijlstra, W. G.; Buursma, A.; Meeuwse-van der Roest, W. P. *Clin. Chem.* **1991**, *37*, 1633–1638.
- (33) Neville, R. G. *Br. Med. J.* **1987**, *294*, 1263–1265.
- (34) Rippmann, C. E.; Nett, P. C.; Popovic, D.; Seifert, B.; Pasch, T.; Spahn, D. R. *J. Clin. Monit.* **1997**, *13*, 373–377.